Evaporative and Convective Instability in the Two-layer Marangoni-Bénard System of Vapor-liquid

Qiu-Sheng Liu[1]*, Rong Liu [1], Zhi-Qiang Zhu[1], Jia-Ping Yan[1], Shu-Ling Chen[2]

[1] *Institute of Mechanics, Chinese Academy of Sciences, Beijing, China 100080*
[2] *Beijing Jiaotong University, Beijing, China 100044*

14 September 2006

Abstract

The effects of liquid evaporation on the interfacial tension-induced convection and instability are studied theoretically and experimentally in present paper. The main purpose of this investigation is to understand the mechanism of convection instability in a thin vapor-liquid layer with a mass exchange surface (interface) where exists the coupling of evaporation phenomenon and Marangoni-Bénard instability. A systematic model of two-layer system consisting of the evaporating liquid layer and vapor-phase layer, heated from below, is studied by linear instability analysis. The thickness of both layers is finite and each layer has an infinite extension in length. The top wall is assumed as a porous medium pervious to vapor, through which the gas phase is passed in a certain velocity in order to control the evaporation flux and vapor pressure. Deformable vapor-liquid interface in the perturbation state are considered, and the influence on the convection instability of the system are analyzed comparatively. Neutral stability curves of the two-layer system are presented for different cases, such as evaporation coefficient, evaporating mass flux, gravity, etc.

1. Introduction

Convection occurring in an infinite horizontal liquid layer, heated from below, has received extensive attention since Bénard [1] observed hexagonal roll cells upon onset of convection in molten spermaceti with a free surface. Rayleigh [2], Pearson [3] analyzed that Bénard convection theoretically. Nield [4] found that buoyancy and surface tension are tightly coupled in Bénard's experiment. Pearson's and Nield's theories can successfully explain the onset of convection in a thin liquid layer without evaporation interface. In Block's works[5] , the qualitative description of the convection evaporating liquid layers has been overlooked. Mechanisms of convection instability induced by the coupling of evaporation and Marangoni effect in thin-liquid layers are still not clear until now.

Evaporative convection is of great interest in engineering because of its importance in modern technologies such as thin-film evaporators, boiling equipments and heat pipes. The evaporative convection leads to interfacial instability where an flat surface becomes undulated when temperature drop across the liquid layer exceeds a critical value.

The evaporation is a complicate phenomenon and it is helpful to separate the different aspect of the problem when we investigate it. For this reason, in previous works[6, 7], most studies on Marangoni-Bénard instability were carried out for single liquid phase systems, and the vapour phase adjacent to the liquid layer was considered as passive. In this case, the dynamics of the thermal and mechanical perturbations in the vapour is neglected. Miller [8] examined the instabilities of an isothermal evaporating interface associated with a moving boundary. Burelbach, Bankoff and Davis [9] investigated the nonlinear stability of evaporating and condensing liquid films. Vapour recoil, thermocapillary and rupture instabilities are discussed in their works. Recently, Ozen and Narayanan [10] proposed a two-sided model that consists of a liquid layer and its own vapour. They only investigated the instabilities of the onset of evaporating. As this case the evaporation flux of unperturbed state is zero, the vapour recoil effect is not taken into account in their discussion. Further more, there is an open question that the Hertz-Knudsen [11] equation is not introduced to the interface boundary conditions and the model is mathematic unenclosed. Chai and Zhang et al [12, 13] studied experimentally the effects of evaporating on Marangoni-Bénard convection in

* Tel.: +86-10-62651167; *E-mail address*: liu@imech.ac.cn

thin liquid layers evaporating at room temperature. In our previous works [14], we discussed the instabilities of the two-sided model with non-deformable vapor-liquid interface.

2. Mathematical model

2.1. Physical situation

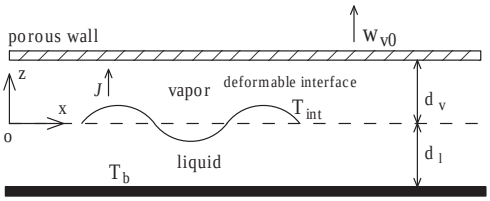

Fig.1. Schematic diagram of definite depth liquid-vapor layer system with a deformable interface.

Here we propose a theoretical model of two-layer evaporating system with a deformable interface, as shown schematically in Fig.1. The physical model consists of a liquid of depth d_l underling its own vapor of depth d_v. Both the top wall and the bottom wall are considered as rigid perfectly conducting boundaries. The top wall is assumed as a porous medium to vapor, through which the vapour phase can pass at a certain velocity. The phase change rate at the interface can be controlled by adjusting the vapour pressure. In unperturbed state, the liquid is evaporating at a certain steady evaporating rate, and it is assumed that there is no convection in vapor layer and evaporating liquid layer. However, the local evaporating velocity is not constant as it can change upon perturbation. The interfacial tension at the interface is considered to be a linear function of temperature: $\sigma = \sigma_0 - \sigma_T(T - T_0)$, where T_0 is the reference temperature of interface. To model interfacial and mass transfer, it is conventional to use the interfacial thermal and chemical potential equilibrium condition.

At the evaporating interface, a kinetic relation like the Hertz-Knudsen law should be used in place of the chemical potential equilibrium condition.

Hertz Knudsen equation [11, 17] predicts a mass flux at the interface proportional the difference between the pressure of the vapour and the saturate pressure of the interface:

$$J = \beta\sqrt{\frac{M}{2\pi RT}}(p_s(T) - p_0(T)) \tag{1}$$

Here β is the evaporation accommodation coefficient, M is the molecular weight of vapor, $p_s(T)$ is the saturation pressure at surface interface temperature T, $p_0(T)$ is the vapor pressure just beyond the interface, R is the universal gas constant.

2.2. Governing equations

The governing equations for each fluid layer are the continuity equation, the energy equation and the Navier-Stokes equations with the Boussinesq approximation [15, 16], i.e., only the densities $\rho_i (i = v, l)$ are dependent of the temperature. The equations used herein are derived in detail in Ref [17] and for this reason their derivation need not be repeated here.

In vapour and liquid phase, the controlling equations are:

$$\frac{\partial u_i}{\partial x} + \frac{\partial w_i}{\partial z} = 0 \tag{2}$$

$$\frac{\partial u_i}{\partial t} + u_i\frac{\partial u_i}{\partial x} + w_i\frac{\partial u_i}{\partial z} = -\frac{1}{\rho_i}\frac{\partial p_i}{\partial x} + \nu_i\nabla^2 u_i \tag{3}$$

$$\frac{\partial w_i}{\partial t} + u_i\frac{\partial w_i}{\partial x} + w_i\frac{\partial w_i}{\partial z} =$$

$$-\frac{1}{\rho_i}\frac{\partial p_i}{\partial z} + \nu_i\nabla^2 w_i - g[1 - \beta_v(T_i - T_{i0})] \tag{4}$$

$$\frac{\partial T_i}{\partial t} + u_i\frac{\partial T_i}{\partial x} + w_i\frac{\partial T_i}{\partial z} = \kappa_i\nabla^2 T_i \tag{5}$$

2.3. Boundary conditions

It is assumed that the bottom and top plate temperatures are kept constant:

$$T_v(d_v) = T_u, T_l(-d_l) = T_b \tag{6}$$

The no-slip condition along the bottom plate:

$$u_l(-d_l) = 0, w_l(-d_l) = 0 \tag{7}$$

The permeable condition of the normal velocity and no-slip condition of the horizontal velocity along the top plate:

$$u_v(d_v) = 0, w_v(d_v) = w_{v0} \tag{8}$$

At the deformable interface, the unknown position of the interface can be described by its variable height $z = \eta(x, t)$. If $\vec{u}_{int}$ denotes the interface velocity, a kinematic relation between $\vec{u}_{int}$ and $\eta(x, t)$ is obtained by $w_{int} = dz/dt$ and $u_{int} = dx/dt$.

The mass balance equation at the interface $z = \eta(x, t)$ is

$$J = \rho_v(\vec{u}_v - \vec{u}_{int}) \cdot \vec{n} = \rho_l(\vec{u}_l - \vec{u}_{int}) \cdot \vec{n} \tag{9}$$

The normal momentum and the tangential momentum balance equations at the interface are:

$$J[\vec{u}]_v^l \cdot \vec{n} + [p - \mathbf{P} \cdot \vec{n} \cdot \vec{n}]_v^l = -2\sigma H \tag{10}$$

$$[\mathbf{P} \cdot \vec{n} \cdot \vec{t}\ ]_v^l = \frac{1}{N}\frac{\partial\sigma}{\partial T}(\frac{\partial T}{\partial x} + \frac{\partial\eta}{\partial x}\frac{\partial T}{\partial z}) \tag{11}$$

The energy balance equation at the interface is:

$$J[|\vec{u} - \vec{u}_{int}|^2]_v^l + J_l - J_v - [\mathbf{P} \cdot (\vec{u} - \vec{u}_{int}) \cdot \vec{n}]_v^l = JL \tag{12}$$

Supposing the thermodynamic equilibrium state is satisfied at the interface, the temperature of the liquid and vapour are continuous:

$$T_v = T_l \tag{13}$$

The Hertz Knudsen relation connecting the evaporation flux and the difference between the saturate pressure of the liquid and the pressure of the vapour just beyond the interface.

$$J = \beta\sqrt{\frac{M}{2\pi RT}}[P_s(T) - p_v(T)] \tag{14}$$

The saturate pressure at a given temperature is given by Clausius-Clapeyron relation:

$$P_s(T) = p_0 \exp[\frac{L}{R}(\frac{1}{T} - \frac{1}{T_0})] \tag{15}$$

The no slip condition at the interface ,The tangential velocity of the liquid and vapour layer is equal.

$$\vec{u}_v \cdot \vec{t} = \vec{u}_l \cdot \vec{t} \tag{16}$$

Here $\vec{n}$ is the unit normal vector, $\vec{t}$ is the unit tangential vector. $2H$ is the surface mean curvature.

2.4. Unperturbed state solution of the system

In the unperturbed state there is no flow in the liquid layer and the evaporation rate is a constant, thus $u_{l0} = w_{l0} = 0$ and $u_{v0} = 0, w_{v0} = w_u$. The unperturbed temperature distribution is closed to be linear at liquid as well as vapor layers.

2.5. Perturbation equations

In a standard way, we apply infinitesimal disturbances to the system as follows:

$$\begin{pmatrix} u_i \\ w_i \\ p_i \\ T_i \\ \eta \end{pmatrix} = \begin{pmatrix} u_{i0} \\ w_{i0} \\ p_{i0} \\ T_{i0} \\ 0 \end{pmatrix} + \begin{pmatrix} u_i' \\ w_i' \\ p_i' \\ T_i' \\ \eta' \end{pmatrix}$$

After we perturb the controlling equations and the boundary conditions, we will and introduce spatial normal perturbations proportional to $exp[\lambda t + ikx]$ into the linearized full governing equations and boundary conditions.

$$\begin{pmatrix} u_i' \\ w_i' \\ T_i' \\ p_i' \\ \eta' \end{pmatrix} = \begin{pmatrix} U_i(z) \\ W_i(z) \\ \Theta_i(z) \\ P_i(z) \\ \eta \end{pmatrix} \exp[\lambda t + ikx]$$

At last, we arrive at the following controlling equations in the domain in dimensionless form.

$$ikU_v + DW_v = 0 \tag{17}$$

$$\lambda\rho^* U_v + w_{v0} DU_v = -ikP_v + \nu^*\rho^*\nabla^2 U_v \tag{18}$$

$$\lambda Pr\rho^* W_v + Prw_{v0} DW_v =$$

$$-PrDP_v + Pr\nu^*\rho^*\nabla^2 W_v + \rho^*\beta^* Ra\Theta_v \tag{19}$$

$$\lambda Pr\Theta_v + Pr\frac{\partial T_{v0}}{\partial z} W_v + Prw_{v0} D\Theta_v = \kappa^*\nabla^2\Theta_v \tag{20}$$

$$ikU_l + DW_l = 0 \tag{21}$$

$$\lambda U_l = -ikP_l + \nabla^2 U_l \tag{22}$$

$$\lambda PrW_l = -PrDP_l + Pr\nabla^2 W_l + Ra\Theta_l \tag{23}$$

$$\lambda Pr\Theta_l + Pr\frac{\partial T_{l0}}{\partial z} W_l = \nabla^2\Theta_l \tag{24}$$

Boundary conditions at the top wall (z=h):

$$U_v = W_v = \Theta_v = 0 \tag{25}$$

and the bottom wall (z=−1):

$$U_l = W_l = \Theta_l = 0 \tag{26}$$

Boundary conditions at the interface (z=0):

$$\rho^*(W_v - \lambda\eta) = W_l - \lambda\eta \tag{27}$$

$$2J_0(W_l - W_v) + P_l - P_v - 2DW_l + 2\mu^* DW_v$$

$$= [k^2\frac{1}{PrCa} + (1-\rho^*)\frac{Ga}{Pr}]\eta \tag{28}$$

$$Pr(DU_l + ikW_l) - Pr\mu^*(DU_l + ikW_l) =$$

$$-ikMa(\Theta_l + \frac{dT_{l0}}{dz}\eta) \tag{29}$$

$$E(W_l - \lambda\eta) - \chi^*\frac{dT_v}{dz} + \frac{dT_l}{dz} = 0 \tag{30}$$

$$U_l = U_v \tag{31}$$

$$\Theta_l + \frac{\partial T_{l0}}{\partial z}\eta = \Theta_v + \frac{\partial T_{v0}}{\partial z}\eta \tag{32}$$

$$W_v - W_l = E_2[E_1^{-1}(\Theta_l + \frac{\partial T_{l0}}{\partial z}\eta) - P_v] \tag{33}$$

Here ν_l/d_l, d_l^2/ν_l, d_l and ΔT are the scaling factors for velocity, time, length and temperature respectively. The layers have non-dimensional depths $h = d_v/d_l$. The dimensionless ratio of the fluid properties are $\kappa^* = \kappa_v/\kappa_l$ (thermal diffusivity), $\beta^* = \beta_v/\beta_l$ (volumetric expansion coefficient), $\chi^* = \chi_v/\chi_l$ (thermal conductivity), $\mu^* = \mu_v/\mu_l$ (dynamic viscosity), $\rho^* = \rho_v/\rho_l$ (density) and $\nu^* = \nu_v/\nu_l$ (kinematical viscosity), respectively. The subscripts v and l refer to the vapor and liquid layers respectively. D is the

dimensionless differential operator d/dz, ∇^2 the operator $D^2 - k^2$, λ the time growth rate, k the dimensionless wavenumber, and dT_{i0}/dz the temperature gradient of fluid-i at the unperturbed state. w_{v0} is the dimensionless evaporation velocity of vapor leaving the interface in the unperturbed state. Ma the Marangoni number defined as $\sigma_T \Delta T d_l/(\mu_l \kappa_l)$, where $\Delta T = T_b - T_{int}$ is the temperature differences in the liquid layer, Ca is the capillary number defined as $Ca = \mu_l \kappa_l/\sigma_0 d_l$, Ga defined as $Ga = g d_l^3/\nu_l \kappa_l$, E is defined as $E = \frac{\rho_l \nu_l \mathcal{L}}{\chi_l \Delta T}$,$E_1$ defined as $E_1 = \frac{\rho_l \nu_l^2 T_0}{\rho_v h_l^2 L \Delta T}$, E_2 defined as $E_2 = \beta\sqrt{\frac{M}{2\pi RT}}\frac{\rho_l - \rho_v}{\rho_v}\frac{\nu_l}{h_l}$, here $\mathcal{L}$ is the evaporation latent heat. Pr the Prandtl number of fluid defined as ν_l/κ_l.

The linear equations (17-24) together with its boundary conditions (25-33) can be discretized by using the spectral numerical method (Tau-Chebyshev).

3. Results and discussion

The water with its own vapor at 100°C is selected in the present study and the depth of the liquid layer is 1mm. The ratios of physical properties (see Ref.[18]) and dimensionless numbers of the liquid-vapor system are ν^* =71.72, ρ^*=6.25×10^{-4}, χ^* =3.68×10^{-2}, κ^*=0.118, Pr=1.78, and Ra=0. The depth ratio of vapour and liquid is h=0.1.

3.1. The cooling effect of the evaporation

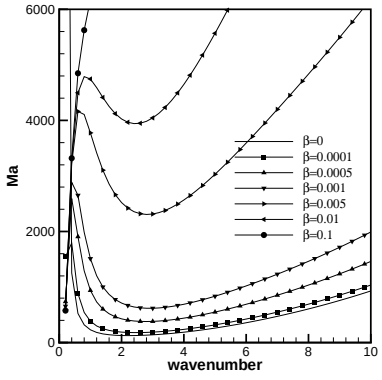

Fig.2. g=0, the vapour liquid depth ratio is 1:10,the critical Marangoni number versus the wavenumber for various evaporation coefficients.

The accommodation evaporating coefficient presents the magnitude of the evaporation at the liquid interface. If there is no evaporation at the interface, the correspondent β is zero. Fig.2. shows the neutral stability curves with different evaporating accommodation coefficient. In the case $\beta = 0$, the amplitude of the perturbed velocity is continuous at the interface. In Fig.2. the system is most unstable for $\beta = 0$. When the evaporating accommodation coefficient is close to zero, the instability of the system is close to be most instable.

According to boundary condition(33), a perturbation of the evaporation velocity will be responsible for a fluctuation of the temperature at the interface. As we know, evaporation will take heat from the interface and cooling the interface. This cooling mechanism may weaken the temperature fluctuation at the interface and make the system more stable.

In Fig.2., The critical Marangoni numbers grows with the β. This means the vapor-liquid system gets more stable with the growing of the β. $\beta \to \infty$ presents a special case. In this case, the liquid-vapor interface is an isothermal boundary and the system is unconditional stable because the Marangoni convection can not be established without the temperature perturbation founded at the interface.

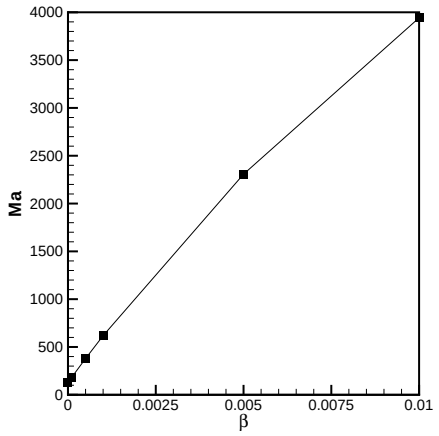

Fig.3. g=0, the vapour liquid depth ratio is 1:10, the critical Marangoni number at large wavenumber versus evaporation coefficients.

Fig.3. shows that the critical Marangoni number and the accommodation evaporation coefficient have approximatively the linear relation.

3.2. The vapour recoil effect

Because mass must be conserved at the interface, a discontinuity in both the fluid velocity normal to the interface is responsible for the change in fluid density during evaporation. Momentum must also be conserved, therefore the discontinuity in velocity results in a downward force on the interface and this force increases with the evaporation rate and with the density of the density ratio of the liquid and vapour phase. Since the interface is deformable, local surface depressions can be produced by the force exerted on the surface by the rapidly departing vapour and this mechanism is called 'differential vapour recoil'. When the system perturbed, it responds according to the dynamical equations. This responds may carry it still further from the original unperturbed state.

Here we will discuss two forms of perturbation at the interface, i.e., a disturbance in the form of a local increase in surface temperature and a disturbance in form of the deflexion of the interface.

The former will increase the local evaporation rate and decrease the local surface tension. The increase in evaporation rate produces a local normal force on the interface and a local depression in the interface is formed. Now the latter form of perturbation arises from the former form.

A deflected interface does not have the uniform temperature at the interface. A trough is at a higher temperature as is it is close to the heat source(the bottom wall) and a crest vice versa. Upon perturbation, a trough is at a temperature higher than the reference temperature, this means that the evaporation will take place at the perturbed state. At a crest where the temperature is colder than that of the reference state, the vapor will condense into its own liquid. A disturbance in the form of a local increase in surface temperature will increase the local evaporation rate and decrease the local surface tension. The increase in evaporation rate produces a local increase in normal force and the result is a local depression at the interface. At this point of the interface, the temperature get hotter for it is closer to the heat source. So the evaporation rate get greater than before and the interface will continue to depress. In a sense, the relation between the perturbation of temperature at the interface and the deflexion of the interface is somewhat like an auto-ampliative mechanism.

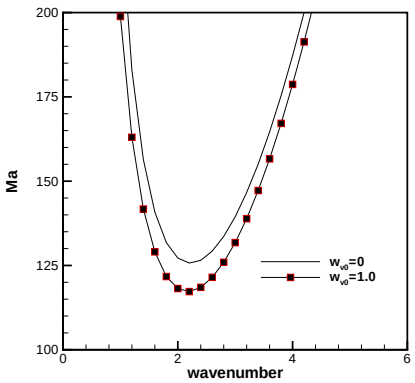

Fig.4. the vapour liquid depth ratio is 1:10 the evaporation coefficient is 0,Marangoni number versus wavenumber

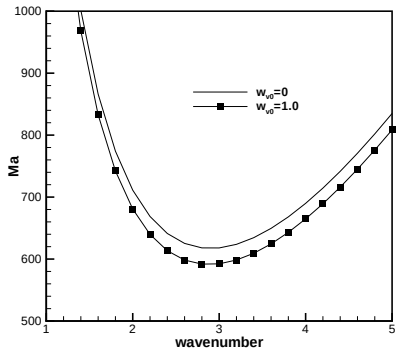

Fig.5. the vapour liquid depth ratio is 1:10 the evaporation coefficient is 0.001,Marangoni number versus wavenumber

In Fig.4, we observe that at all wavenumbers the system with zero evaporation velocity is instable than that with non-zero evaporation velocity, as the Marangoni number of $w_{v0} = 0$ is greater than that of $w_{v0} = 1.0$. This means the vapour recoil effect can get the system more instable.

Fig.5,the accommodation evaporation efficient is 0.001. The system with zero evaporation velocity is more instable. Comparing Fig.2 to Fig.3, we find that the critical Marangoni number with $\beta = 0$ is more instable than that with $\beta = 0.001$, when the evaporating velocity is same.

If the steady evaporation rate is high enough to overcoming the stabilizing effect of the gravity and the cooling effect of the evaporation, the vapor recoil effect is capable to produce convection in the liquid layer. As we know, the accommodation evaporation efficient presents the cooling ability. The greater is β , the more temperature difference across the liquid layer is need to drive the convection in it.

3.3. The influence of the gravity

In many laboratory situations, gravity plays an important role.

Gravity has two kinds of effect on the system. One is the Rayleigh effect(Buoyancy-driven) and the other is the interfacial effect. Buoyancy-driven convection occurs when a fluid is subject to a temperature gradient perpendicular to the layer interface and there is a variation of density with respect to temperature. Supposing the temperature of the lower wall is hotter than that of the interface, the fluid near the interface is heavier than the fluid at the bottom wall, for density typically decreases with an increase in temperature. Imagine a mechanical perturbation driving down a fluid element, as the density of this fluid element is greater than its environment, it will proceed downward. Fluid form below will move upward due to mass conservation. This motion continues unless the viscosity and thermal diffusivity are too high to

abate it until this perturbation die out.

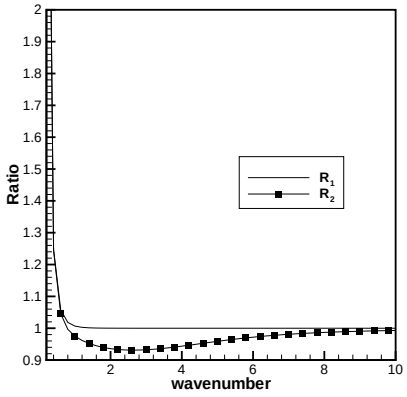

Fig.6. The depth ratio is 1:10, evaporation coefficient is 0.01, the ratio of R_1 and R_1 versus wavenumber.

The Rayleigh effect is very obvious and simple, as discussed above, it makes the system instable. However, this effect can be avoid supposing the liquid layer is very thin. In this case, gravity simply pulls the perturbed interface back to its original position and plays a stabilizing effect at all wavenumbers. The interfacial effect of gravity makes the system stable. In Fig.6. R_1 and R_2 are great than 1 at the small wavenumbers, this means the interfacial effect of the gravity get the system more stable. It is similar to that of the one layer liquid system, the interfacial effect of gravity on the system is more obvious at small wavenumbers and almost has no influence at the large wavenumbers.

The Rayleigh effect is depicted by the curve labeled R_2 in Fig.6. The Rayleigh effect is not operative at all wave numbers. AT the wavenumber range $2.0-8.0$, R_2 is less than 1. At large enough wavenumber, the buoyancy driven mechanism is swept away by the Maranogni effect and merges with the unity line.

4. Conclusion

In our present study, the vapor recoil effect has destabilization mechanism to the system, and the cooling effect of the evaporation has stabilization mechanism to the system. The Rayleigh effect stabilizes the system whereas the interfacial effect of gravitation destabilizes it.

Reference

[1] Bénard H. Les Tourbillons Cellulaires dans une Nappe Liquide. *Rev Gen Sci Pures Appl,* 1900, 11: 1261∼1271

[2] Rayleigh L. On Convection Currents in a Horizontal Layer of Fluid, When the Higher Temperature Is on the Under Side. *Phil Mag,* 1916, 32(6): 529∼546

[3] Pearson JRA. On Convection Cells Induced by Surface Tension. *J Fluid Mech,* 1958, 4: 489∼500

[4] Nield DA. Surface Tension as the Cause of Bénard Cells and Surface Deformation in a Liquid Film. *J Fluid Mech,* 1964, 19: 341∼352

[5] Block MJ. Surface Tension as the Cause of Bénard Cells and Surface Tension Deformation in a Liquid Film. *Nature,* 1956, 178: 650∼651

[6] Palmer H J 1976 *J. Fluid Mech.* **75** 487

[7] Prosperetti A and Plesset M S 1984 *Phys. Fluids* **7(7)** 1590

[8] Miller CA. Stability of moving surface in fluid systems with heat and mass transport. Part II-Combined effects of transport and density difference between phases. *AIChE J.* 1973, 19: 909∼915.

[9] Burelbach JP, Bankoff SG, Davis SH. Nonlinear Stability of Evaporating/Condensing Liquid Films. *J Fluid Mech,* 1988, 195: 463∼494

[10] Ozen O, Narayanan R. The physics of evaporative and convective instabilities in bilayer systems: Linear theory. *Phys. Fluids.* 2004, 16(12): 4644∼4652.

[11] Kennard E K 1938 *Kinetic Theory of gases* (New York:McGraw-Hill)

[12] Zhang N and Chao D F 1999 *Int. Comm. Heat Mass Transfer* **26(8)** 1069

[13] An-Ti Chai and Nengli Zhang 1998 *Experiment Heat Transfer* **11** 187

[14] Liu R, Liu QS, Hu WR. Marangoni-Bénard Instability with the Exchange of Evaporation at Liquid-vapor interface. *Chin Phys Lett,* 2005, 22(2): 402∼405

[15] Batchlor G K 1970 *An Introdution to Fluid Dynamics* (Cambridge:Cambridge University Press)

[16] Liu Q S, Roux B and Velarde M G 1998 *Int. J. Heat Mass Transfer* **41** 1499

[17] Colinet P, Legros J C and Velarde M G 2001 *Nonlinear Dynamics of Surface-Tension-Driven Instabilities.* (Berlin:Wiley-VCH Verlag Berlin GmbH)

[18] Lide D R and Kehiaian H V 1994 *CRC Handbook of Thermophysical and Thermochemical Data* (Boca Raton:DRC Press)